

## Optimal light storage with full pulse-shape control

Irina Novikova,<sup>1</sup> Nathaniel B. Phillips,<sup>1</sup> and Alexey V. Gorshkov<sup>2</sup>

<sup>1</sup>*Department of Physics, College of William & Mary, Williamsburg, Virginia 23185, USA*

<sup>2</sup>*Department of Physics, Harvard University, Cambridge, Massachusetts 02138, USA*

(Received 13 May 2008; published 20 August 2008)

We experimentally demonstrate optimal storage and retrieval of light pulses of arbitrary shape in atomic ensembles. By shaping auxiliary control pulses, we attain efficiencies approaching the fundamental limit and achieve precise retrieval into any predetermined temporal profile. Our techniques, demonstrated in warm Rb vapor, are applicable to a wide range of systems and protocols. As an example, we present their potential application to the creation of optical time-bin qubits and to controlled partial retrieval.

DOI: [10.1103/PhysRevA.78.021802](https://doi.org/10.1103/PhysRevA.78.021802)

PACS number(s): 42.50.Gy, 32.70.Jz, 42.50.Md

Quantum memory for light is essential for the implementation of long-distance quantum communication [1] and of linear optical quantum computation [2]. Both applications put forth two important requirements for quantum memory: (i) the memory efficiency is high (i.e., the probability of losing a photon during storage and retrieval is low) and (ii) the retrieved photonic wave packet has a well-controlled shape to enable interference with other photons. In this Rapid Communication, we report on an experimental demonstration of this full optimal control over light storage and retrieval: by shaping an auxiliary control field, we store an incoming coherent signal pulse of arbitrary shape and then retrieve it into any desired output pulse shape with the maximum efficiency possible for the given memory. While our results are obtained in warm Rb vapor using electromagnetically induced transparency (EIT) [3,4], the presented procedure is universal [5] and applicable to a wide range of systems, including ensembles of cold atoms [6–8] and solid-state impurities [9,10], as well as to other light storage protocols (e.g., the far-off-resonant Raman scheme [11]). Although our experiment uses weak classical pulses, the linearity of the corresponding equations of motion [5] allows us to expect that our results will be applicable to quantum states confined to the mode defined by the classical pulse.

We consider the propagation of a weak signal pulse in the presence of a strong classical control field in a resonant  $\Lambda$ -type ensemble under EIT conditions, as shown in Fig. 1(a). An incoming signal pulse propagates with slow group velocity  $v_g$ , which is uniform throughout the medium and is proportional to the intensity of the control field,  $v_g \approx 2|\Omega|^2/(\alpha\gamma) \ll c$  [12]. Here,  $\Omega$  is the control Rabi frequency,  $\gamma$  is the decay rate of the optical polarization, and  $\alpha$  is the absorption coefficient, so that  $\alpha L$  is the optical depth of the atomic medium of length  $L$ . For quantum memory applications, a signal pulse can be “stored” (i.e., reversibly mapped) onto a collective spin excitation of an ensemble (spin wave) by reducing the control intensity to zero [12]. In the limit of infinitely large optical depth and negligible ground-state decoherence, any input pulse can be converted into a spin wave and back with 100% efficiency, satisfying requirement (i). Under the same conditions, any desired output pulse shape can be easily obtained by adjusting the control field power (and hence the group velocity) as the pulse exits the medium, in accordance with requirement (ii). However, most current experimental realizations of ensemble-

based quantum memories operate at limited optical depth  $\alpha L \lesssim 10$  due to various constraints [4,6–10]. At finite  $\alpha L$ , losses limit the maximum achievable memory efficiency to a value below 100%, making efficiency optimization and output-pulse shaping important and nontrivial [5].

In this Rapid Communication, we experimentally demonstrate the capability to satisfy both quantum memory requirements in an ensemble with a limited optical depth. Specifically, by adjusting the control field envelopes for several arbitrarily selected input pulse shapes, we demonstrate precise retrieval into any desired output pulse shape with experimental memory efficiency very close to the fundamental limit [5,13]. This ability to achieve maximum efficiency for any input pulse shape is crucial when optimization with respect to the input pulse [14] is not applicable (e.g., if the photons are generated by parametric down-conversion [15]). At the same time, control over the outgoing mode, with precision far beyond early attempts [16–19], is essential for experiments based on the interference of photons stored under

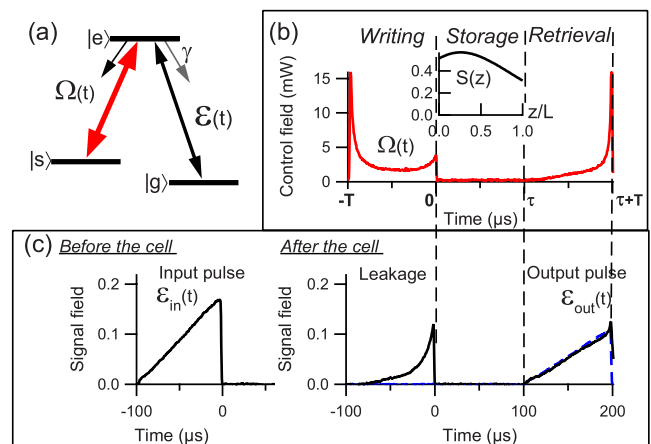


FIG. 1. (Color online) (a) Schematic of the three-level  $\Lambda$  interaction scheme. Control (b) and signal (c) fields in pulse-shape-preserving storage of a “positive-ramp” pulse using a calculated optimal control field envelope  $\Omega(t)$ . During the writing stage ( $t < 0$ ), the input pulse  $\mathcal{E}_{in}(t)$  is mapped onto the optimal spin wave  $S(z)$  [inset in (b)], while a fraction of the pulse escapes the cell (leakage). After a storage time  $\tau$ , the spin wave  $S(z)$  is mapped into an output signal pulse  $\mathcal{E}_{out}(t)$  during the retrieval stage. The dashed blue line in (c) shows the target output pulse shape.

different experimental conditions (e.g., in atomic ensembles with different optical depths) or stored a different number of times. In addition, control over output pulse duration may also allow one to reduce sensitivity to noise (e.g., jitter). It is important to note that shaping the output mode via the control pulse avoids additional losses that would be present if one were to post-process the retrieved photon with an electro-optical modulator [20].

The experimental setup is described in detail in Ref. [21]. We phase-modulated the output of an external cavity diode laser to produce modulation sidebands separated by the ground-state hyperfine splitting of  $^{87}\text{Rb}$  ( $\Delta_{\text{HF}}=6.835$  GHz). For this experiment, we tuned the zeroth order (control field) to the  $F=2 \rightarrow F'=2$  transition of the  $^{87}\text{Rb}$   $D_1$  line, while the +1 modulation sideband played the role of the signal field and was tuned to the  $F=1 \rightarrow F'=2$  transition. The amplitudes of the control and signal fields were controlled independently by simultaneously adjusting the phase modulation amplitude (by changing the rf power sent to the electro-optical modulator) and the total intensity in the laser beam (using an acousto-optical modulator). Typical peak control field and signal field powers were 18 mW and 50  $\mu\text{W}$ , respectively. The  $-1$  modulation sideband was suppressed to 10% of its original intensity using a temperature-tunable Fabri-Perot étalon. In the experiment, we used a cylindrical Pyrex cell (length and diameter were 75 mm and 22 mm, respectively) containing isotopically enriched  $^{87}\text{Rb}$  and 30 Torr Ne buffer gas, mounted inside three-layer magnetic shielding and maintained at the temperature of 60.5  $^\circ\text{C}$ , which corresponds to an optical depth of  $\alpha L=24$ . The laser beam was circularly polarized and weakly focused to  $\approx 5$  mm diameter inside the cell. We found the typical spin-wave decay time to be  $1/(2\gamma_s) \approx 500$   $\mu\text{s}$ , most likely arising from small, uncompensated remnant magnetic fields. The duration of pulses used in the experiment was short enough for the spin decoherence to have a negligible effect during writing and retrieval stages and to cause a modest reduction of the efficiency  $\propto \exp(-2\gamma_s\tau)=0.82$  during the storage time  $\tau=100$   $\mu\text{s}$ . For the theoretical calculations, we model the  $^{87}\text{Rb}$   $D_1$  line as a homogeneously broadened [22]  $\Lambda$  system with no free parameters, as in Ref. [14] (see Ref. [21] for details).

An example of optimized light storage with controlled retrieval is shown in Figs. 1(b) and 1(c). In this measurement, we chose the input pulse  $\mathcal{E}_{\text{in}}(t)$  [23] to be a “positive ramp.” According to theory [5,13], the maximum memory efficiency is achieved only if the input pulse is mapped onto a particular optimal spin wave  $S(z)$ , unique for each  $\alpha L$ . The calculated optimal spin wave for  $\alpha L=24$  is shown in the inset in Fig. 1(b). Then, we used the method described in Ref. [13] to calculate the *writing* control field  $\Omega(t)$  ( $-T < t < 0$ ) that maps the incoming pulse onto the optimal spin wave  $S(z)$ . To calculate the *retrieval* control field  $\Omega(t)$  ( $\tau < t < \tau+T$ ) that maps  $S(z)$  onto the target output pulse  $\mathcal{E}_{\text{tgt}}(t)$ , we employ the same writing control calculation together with the following time-reversal symmetry of the optimized light storage [5,13,14]. A given input pulse, stored using its optimal writing control field, is retrieved in the time-reversed and attenuated copy of itself [ $\mathcal{E}_{\text{out}}(t) \propto \mathcal{E}_{\text{in}}(\tau-t)$ ] when the time-reversed control is used for retrieval [ $\Omega(t)=\Omega(\tau-t)$ ]. Thus the control field that retrieves

the optimal spin wave  $S(z)$  into  $\mathcal{E}_{\text{tgt}}(t)$  is the time-reversed copy of the control that stores  $\mathcal{E}_{\text{tgt}}(\tau-t)$  into  $S(z)$ . As shown in Figs. 1(b) and 1(c), we used this method to achieve pulse-shape-preserving storage and retrieval, i.e., the target output pulse was identical to the input pulse (“positive ramp”). The measured output pulse [solid black line in Fig. 1(c)] matches very well the target shape (dashed blue line in the same figure). This qualitatively demonstrates the effectiveness of the proposed control method.

To describe the memory quantitatively, we define memory efficiency  $\eta$  as the probability of retrieving an incoming photon after some storage time or, equivalently, as the energy ratio between retrieved and initial signal pulses:

$$\eta = \frac{\int_{\tau}^{\tau+T} |\mathcal{E}_{\text{out}}(t)|^2 dt}{\int_{-T}^0 |\mathcal{E}_{\text{in}}(t)|^2 dt}. \quad (1)$$

To characterize the quality of pulse shape generation, we define an overlap integral  $J^2$  as [24]

$$J^2 = \frac{|\int_{\tau}^{\tau+T} \mathcal{E}_{\text{out}}(t) \mathcal{E}_{\text{tgt}}(t) dt|^2}{\int_{\tau}^{\tau+T} |\mathcal{E}_{\text{out}}(t)|^2 dt \int_{\tau}^{\tau+T} |\mathcal{E}_{\text{tgt}}(t)|^2 dt}. \quad (2)$$

The measured memory efficiency for the experiment in Fig. 1 is  $0.42 \pm 0.02$ . This value closely approaches the predicted highest memory efficiency of 0.45 for  $\alpha L=24$  [5,13], corrected to take into account the spin-wave decay during the storage time. The measured value of the overlap integral between the output and the target is  $J^2=0.987$ , which indicates little distortion in the retrieved pulse shape.

The definitions of efficiency  $\eta$  and overlap integral  $J^2$  are motivated by quantum information applications. Storage and retrieval of a single photon in a nonideal passive quantum memory produces a mixed state that is described by a density matrix  $\rho=(1-\eta)|0\rangle\langle 0|+\eta|\phi\rangle\langle\phi|$  [25], where  $|\phi\rangle$  is a single-photon state with envelope  $\mathcal{E}_{\text{out}}(t)$  and  $|0\rangle$  is the vacuum state. Then the fidelity between the target single-photon state  $|\psi\rangle$  with envelope  $\mathcal{E}_{\text{tgt}}(t)$  and the single-photon state  $|\phi\rangle$  is given by the overlap integral  $J^2$  [Eq. (2)], while  $F=\langle\psi|\rho|\psi\rangle=\eta J^2$  is the fidelity of the output state  $\rho$  with respect to the target state  $|\psi\rangle$ . The overlap integral  $J^2$  is also an essential parameter for optical quantum computation and communication protocols [1,2], since  $(1-J^2)/2$  is the coincidence probability in the Hong-Ou-Mandel [26] interference between photons  $|\psi\rangle$  and  $|\phi\rangle$  [24]. One should be cautious in directly using our classical measurements of  $\eta$  and  $J^2$  to predict fidelity for single-photon states because single photons may be sensitive to imperfections that do not significantly affect classical pulses. For example, four-wave mixing processes may reduce the fidelity of single-photon storage, although our experiments [21] found these effects to be relatively small at  $\alpha L < 25$ .

Figure 2 shows more examples of optimal light storage with full output-pulse-shape control. For this experiment, we stored either of two randomly selected input signal pulse shapes—a Gaussian and a “negative ramp”—and then retrieved them either into their original wave forms [(a),(d)] or into each other [(b),(c)]. Memory efficiency  $\eta$  and overlap integral  $J^2$  are shown for each graph. Notice that the efficiencies for all four input-output combinations are very similar

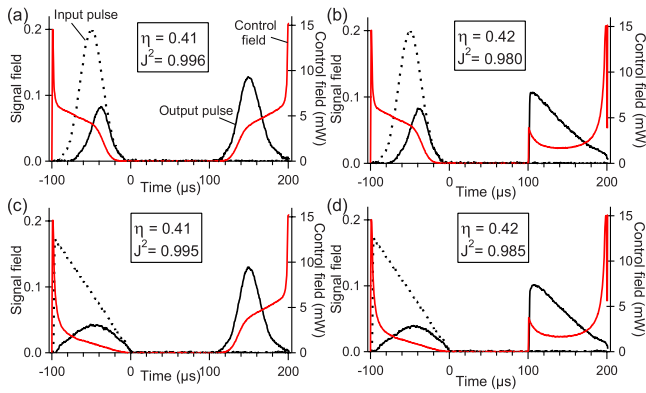


FIG. 2. (Color online) An input Gaussian pulse was optimally stored and retrieved either into its original pulse shape (a) or into a ramp pulse shape (b). Similarly, the incoming ramp pulse was optimally stored and retrieved into a Gaussian (c) or into an identical ramp (d). Input and output signal pulses are shown as dotted and solid black lines, respectively, while the optimal control fields are shown as solid red lines.

( $0.42 \pm 0.02$ ) and agree well with the highest achievable efficiency (0.45) for the given optical depth  $\alpha L = 24$ . The overlap integrals are also very close to 1, revealing an excellent match between the target and retrieved signal pulse shapes. Note that different input pulses stored using corresponding (different) optimized writing control fields but retrieved using identical control fields [pairs (a),(c) and (b),(d)] had identical output envelopes, very close to the target one. This observation, together with the fact that the measured memory efficiency is close to the fundamental limit, suggests that indeed different initial pulses were mapped onto the same optimal spin wave. This indirectly confirms our control not only over the output signal light field, but also over the spin wave.

Our full control over the outgoing pulse shape opens up an interesting possibility to convert a single photon into a

so-called “time-bin” qubit—a single-photon excitation delocalized between two time-resolved wave packets (bins). The state of the qubit is encoded in the relative amplitude and phase between the two time bins [27]. Such time-bin qubits are advantageous for quantum communication since they are insensitive to polarization fluctuations and depolarization during propagation through optical fibers [27]. We propose to efficiently convert a single photon with an arbitrary envelope into a time-bin qubit by optimally storing the photon in an atomic ensemble and then retrieving it into a time-bin output envelope with well-controlled relative amplitude and phase using a customized retrieval control field.

To illustrate the proposed output pulse shaping, in Fig. 3, we demonstrate storage of two different classical input pulses (a Gaussian and a positive ramp), followed by retrieval into a time-bin-like classical output pulse, consisting of two distinct Gaussian pulses  $g_{1,2}(t)$  with controllable relative amplitude and delay. We obtained the target output independently of what the input pulse shape was. We also attained the same memory efficiency as before ( $0.41 \pm 0.02$ ) for all linear combinations. Also, regardless of the input, the output pulse shapes matched the target envelopes very well, as characterized by the value of the overlap integral close to unity,  $J^2 = 0.98 \pm 0.01$ . We also verified that the envelopes of the two retrieved components of the output pulse were nearly identical by calculating the overlap integral  $J^2(g_1, g_2)$  between the retrieved bins  $g_1$  and  $g_2$ . This parameter is important for applications requiring interference of the two qubit components [27]. The average value of  $J^2(g_1, g_2) = 0.94 \pm 0.02$  was consistently high across the full range of target outputs. The relative phase of the two qubit components can be adjusted by controlling the phase of the control field during retrieval. The demonstrated control over the amplitude ratio and shape of the two output pulses is essential for achieving high-fidelity time-bin qubit generation. Our scheme is also immediately applicable to high-fidelity partial retrieval of the spin wave [16], which forms the basis for a recent promising quantum communication protocol [28].

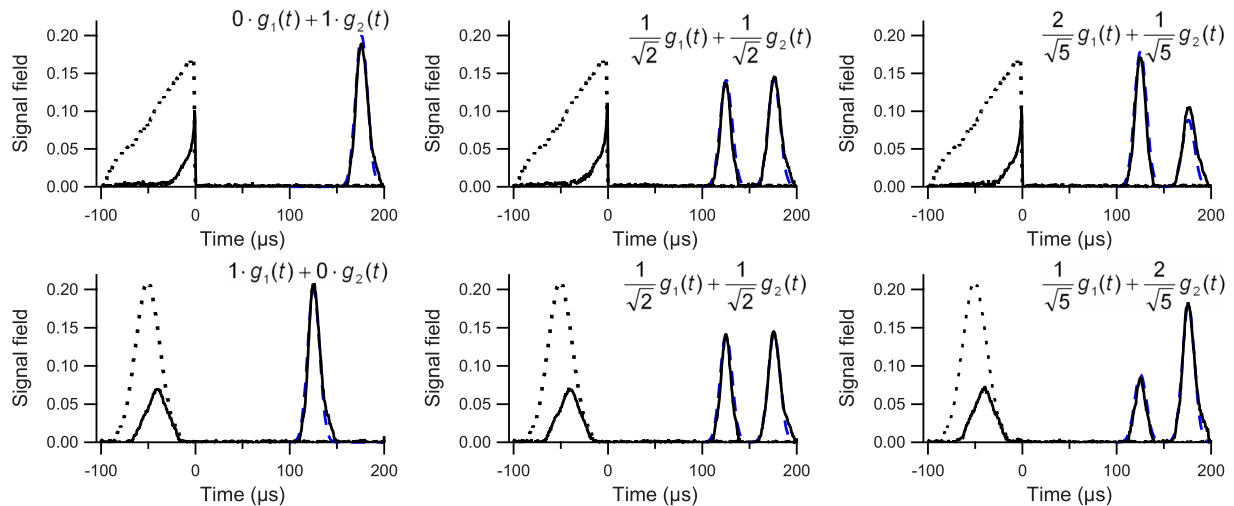


FIG. 3. (Color online) Examples of storage of signal input pulses with Gaussian and triangular envelopes, followed by retrieval in a linear combination of two time-resolved Gaussian pulse shapes  $g_1(t)$  and  $g_2(t)$ . Input and output signal fields are shown as dotted and solid black lines, respectively. Dashed blue lines show the target envelopes.

To conclude, we have reported the experimental demonstration of optimal storage and retrieval of arbitrarily shaped signal pulses in an atomic vapor at an optical depth  $\alpha L=24$  by using customized writing control fields. Our measured memory efficiency is close to the highest efficiency possible at that optical depth. We also demonstrate full precision control over the retrieved signal pulse shapes, achieved by shaping the retrieval control field. A high degree of overlap between the retrieved and target pulse shapes was obtained (overlap integral  $J^2=0.98-0.99$ ) for all input and target pulse shapes tested in the experiments. We also demonstrated the potential application of the presented technique to the creation of optical time-bin qubits and to controlled partial retrieval. Finally, we observed excellent agreement between our experimental results and theoretical modeling. The

optimal storage and pulse-shape control presented here are applicable to a wide range of experiments, since the underlying theory applies to other experimentally relevant situations such as ensembles enclosed in a cavity [8,25], the off-resonant regime [5,13,25], nonadiabatic storage (i.e., storage of pulses of high bandwidth) [29], and ensembles with inhomogeneous broadening [30], including Doppler broadening [4] and line broadening in solids [31]. Thus, we expect this pulse-shape control to be indispensable for applications in both classical [32] and quantum optical information processing.

The authors would like to thank M. D. Lukin, L. Jiang, A. S. Sørensen, P. Walther, and R. L. Walsworth for useful discussions. This research was supported by the NSF, the Jeffress Memorial Trust, and the College of William & Mary.

- 
- [1] L. M. Duan *et al.*, *Nature (London)* **414**, 413 (2001).  
 [2] P. Kok *et al.*, *Rev. Mod. Phys.* **79**, 135 (2007).  
 [3] M. D. Lukin, *Rev. Mod. Phys.* **75**, 457 (2003).  
 [4] M. D. Eisaman *et al.*, *Nature (London)* **438**, 837 (2005).  
 [5] A. V. Gorshkov, A. Andre, M. Fleischhauer, A. S. Sorensen, and M. D. Lukin, *Phys. Rev. Lett.* **98**, 123601 (2007).  
 [6] T. Chanelière *et al.*, *Nature (London)* **438**, 833 (2005).  
 [7] K. S. Choi *et al.*, *Nature (London)* **452**, 67 (2008).  
 [8] J. Simon, H. Tanji, J. K. Thompson, and V. Vuletic, *Phys. Rev. Lett.* **98**, 183601 (2007).  
 [9] A. L. Alexander, J. J. Longdell, M. J. Sellars, and N. B. Manson, *Phys. Rev. Lett.* **96**, 043602 (2006).  
 [10] M. U. Staudt *et al.*, *Phys. Rev. Lett.* **98**, 113601 (2007).  
 [11] A. E. Kozhekin, K. Mølmer, and E. Polzik, *Phys. Rev. A* **62**, 033809 (2000).  
 [12] M. Fleischhauer and M. D. Lukin, *Phys. Rev. Lett.* **84**, 5094 (2000); *Phys. Rev. A* **65**, 022314 (2002).  
 [13] A. V. Gorshkov, A. Andre, M. D. Lukin, and A. S. Sorensen, *Phys. Rev. A* **76**, 033805 (2007).  
 [14] I. Novikova *et al.*, *Phys. Rev. Lett.* **98**, 243602 (2007).  
 [15] J. S. Neergaard-Nielsen *et al.*, *Opt. Express* **15**, 7940 (2007).  
 [16] C. Liu, Z. Dutton, C. H. Behroozi, and L. V. Hau, *Nature (London)* **409**, 490 (2001).  
 [17] A. K. Patnaik, F. L. Kien, and K. Hakuta, *Phys. Rev. A* **69**, 035803 (2004).  
 [18] M. D. Eisaman *et al.*, *Phys. Rev. Lett.* **93**, 233602 (2004).  
 [19] S. Du, P. Kolchin, C. Belthangady, G. Y. Yin, and S. E. Harris, *Phys. Rev. Lett.* **100**, 183603 (2008).  
 [20] P. Kolchin, C. Belthangady, Sh. Du, G. Y. Yin, and S. E. Harris, e-print arXiv:0808.0230.  
 [21] N. B. Phillips, A. V. Gorshkov, and I. Novikova, *Phys. Rev. A* **78**, 023801 (2008).  
 [22] The homogeneous pressure broadened width  $2\gamma \approx 2\pi \times 300$  MHz of the optical transition was comparable to the Doppler broadening.  
 [23] Throughout the paper, all control and signal envelopes are assumed to be real. Also, in all experimental data plots, all signal pulses are shown in the same scale and all input pulses are normalized to have the same unit area  $\int_{-T}^0 |\mathcal{E}_{\text{in}}(t)|^2 dt = 1$ , where  $t$ , is time in  $\mu\text{s}$ .  
 [24] R. Loudon, *The Quantum Theory of Light* (Oxford University Press, New York, 2000).  
 [25] A. V. Gorshkov, A. Andre, M. D. Lukin, and A. S. Sorensen, *Phys. Rev. A* **76**, 033804 (2007).  
 [26] C. K. Hong, Z. Y. Ou, and L. Mandel, *Phys. Rev. Lett.* **59**, 2044 (1987).  
 [27] J. Brendel, N. Gisin, W. Tittel, and H. Zbinden, *Phys. Rev. Lett.* **82**, 2594 (1999).  
 [28] N. Sangouard *et al.*, *Phys. Rev. A* **77**, 062301 (2008).  
 [29] A. V. Gorshkov, T. Calarco, M. D. Lukin, and A. S. Sorensen, *Phys. Rev. A* **77**, 043806 (2008).  
 [30] A. V. Gorshkov, A. Andre, M. D. Lukin, and A. S. Sorensen, *Phys. Rev. A* **76**, 033806 (2007).  
 [31] B. Kraus *et al.*, *Phys. Rev. A* **73**, 020302(R) (2006).  
 [32] R. S. Tucker, P. S. Ku, and C. J. Chang-Hasnain, *J. Lightwave Technol.* **23**, 4046 (2005).